Penerbit Akademia Baru

Journal of Advanced Research in Fluid Mechanics and Thermal Sciences

Journal homepage: www.akademiabaru.com/arfmts.html
ISSN: 2289-7879

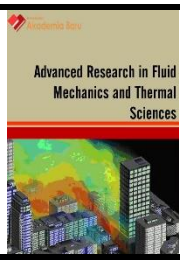

Pitting Hole Evaluation by Active Infrared Thermography in Stainless Steel 304

Open Access

Maznan Ismon[1,2,*] Muhammad Danial Jamalludin[1], Izzuddin Zaman@Bujang[1,2], Nor Azali Azmir[1,2], Rosli Asmawi[2], Mohamad Farid Sies[2], Mohd Nazrul Roslan[3], Zulhairi Ibrahim[4]

[1] The Noise and Vibration Analysis Research Group (NOVIA), Faculty of Mechanical and Manufacturing Engineering, Universiti Tun Hussein Onn Malaysia, Batu Pahat, Johor, Malaysia
[2] Department of Engineering Mechanics (JKM), Faculty of Mechanical and Manufacturing Engineering, Universiti Tun Hussein Onn Malaysia, Batu Pahat, Johor, Malaysia.
[3] Department of Mechanical and Engineering Technology, Faculty of Engineering Technology, Universiti Tun Hussein Onn Malaysia, Batu Pahat, Johor, Malaysia
[4] Perintis Kembara Sdn Bhd, 11-1, Jalan 2A/27A, Seksyen 1, Wangsa Maju, 53300 Kuala Lumpur, Malaysia

ARTICLE INFO

Article history:
Received 31 November 2019
Received in revised form 9 January 2020
Accepted 9 January 2020
Available online 25 March 2020

ABSTRACT

Nowadays, infrared thermography technique is widely use in an engineering study to inspect various types of problem. In this experiment, active infrared thermography method is applied to overcome the constraint locating pitted inside pipe. The main purpose of this experiment is to examine the location of pitted occur in the stainless steel 304 and at the same time to identify the transient effect on the pipe against the duration of time radiation exposed. This experiment uses two unit of spotlight as sources of heat to emit radiation energy to the surface of the pipe. A FLIR T640 thermography camera was used to record the thermal contrast of the pipe in real time using FLIR Tools+ software installs in the laptop. This experiment was tested at normal surrounding temperature. All of the temperature data is then interpreted into contour graph by using Microsoft Excel to see the defect area based on temperature distribution. Based on the result, the most significant temperature drops within highest gradient observed at cooling phase are within 7s, 2s and 1s interval for 10s, 20s and 30s of radiation exposure respectively. The time of the pitted to appear is related to the exposure time of the radiation. The finding of this experiment shows that short duration time of radiation exposure will give the longer time interval of significant gradient to appear. Therefore, this experiment proves that infrared thermography is one of the non- destructive testing methods that can be used in inspecting the pipeline.

Keywords:
Active Infrared thermography; non-destructive test; pitting; corrosion; FLIR tools

* *Corresponding author.*
E-mail address: maznan@uthm.edu.my (Maznan Ismon)

https://doi.org/10.37934/arfmts.68.1.114124

1. Introduction

Pitting in term of corrosion only attack the portion of the metal and form hole to the metal structure. Basically, pitting has its own shape such as vertical, horizontal, wide and shallow. All this shape can be determined by metallography process where the pitted cross section will take and undergo this process. Another method to detect pitting inside the surface is by using thermography process.

Thermography is measure either in two ways, using passive thermography method or active thermography method. Using passive thermography, radiation of the object will be measured without any external heat source of heat supply. Meanwhile, in active thermography, the target object is exposed to the external heat source.

Hence, in this study stainless steel 304 is used as a subject while the main tool using in identifying the pitted is FLIR T640 [1]. This experiment proposed an active thermography method where two spotlights with a power of 500 watt each acting as a heat source transmit to the subject to form thermal difference.

Corrosion has their several types of defects need to be identified, when the type of corrosion had detected it will easier to find out the cause. Example of corrosion are galvanic corrosion [2], microbial corrosion defect [3], high- temperature corrosion, crevise corrosion and pitting corrosion [4].

1.1 Thermography Field

Infrared thermography (IRT) is a new era of the invention in science. This process is non-contact measurement devices where it can process into thermal information, due to the advantages of IRT it has been using nowadays in many fields, for example in building survey [5], machine maintenance [6], health and animal monitoring [7] and electrical component. Monitoring health performance of an electric motor and also gearbox operating is also part of the IRT capability [8], locating internal pipe defect [9] and welding external defect [10].

1.2 Emissivity

Infrared thermography is a type of radiation energy that emitted by molecules. Emissivity has the maximum value of 1 and no unit. Table 1 shows the value of emissivity for a different material.

Table 1
The value of emissivity based on different material [11]

No.	Types of material	The value of emissivity, ε <1
1.	Aluminum	0.83
2.	Carbon	0.95
3.	Copper oxidized	0.78
4.	Iron Cast	0.64
5.	Iron Rusty	0.69
6.	Stainless Steel oxidizes	0.85
7.	Steel Oxidized	0.79

1.3 Stainless Steel 304 (SS304)

This metal has their special properties with high strength, besides it also has quite a resistance and have excellent formability, therefore, 304 stainless steel is using in many applications.

While choosing a specific review of stainless steel, it is good to consider the essential properties required, Figure 1 shows the physical properties of stainless steel 304.

Density, lbs./in.^{3} (g/cm^3)	0.29 (8.03)
Electrical Resistivity, μΩ•in. (μΩ•cm) 68 °F (20 °C) 1200 °F (659 °C)	 28.4 (72) 45.8 (116)
Thermal Conductivity, BTU/hr./ft./°F (W/m/K)	
212 °F (100 °C)	9.4 (16.2)
932 °F (500 °C)	12.4 (21.4)
Mean Coefficient of Thermal Expansion, in./in./°F (μm/m/K)	
32 – 212 °F (0 – 100 °C)	9.4 x 10^{-6} (16.9)
32 – 600 °F (0 – 315 °C)	9.9 x 10^{-6} (17.3)
32 – 1000 °F (0 – 538 °C)	10.2 x 10^{-6} (18.4)
32 – 1200 °F (0 – 649 °C)	10.4 x 10^{-6} (18.7)
Modulus of Elasticity, ksi. (MPa)	
in tension	28.0 x 10^3 (193 x 10^3)
in torsion	11.2 x 10^3 (78 x 10^3)
Magnetic Permeability Annealed, (H/m at 200 Oersteds)	 1.02 max.
Specific Heat, BTU/lbs./°F (kJ/kg/K) 32 – 212 °F (0 – 100 °C)	 0.12 (0.50)
Melting Range, °F (°C)	2550 – 2650 (1399 – 1454)

Fig. 1. Physical properties of stainless steel 304 [12]

1.4 Heat Transfer

Heat is the form of thermal energy that can be transferred from one system to the other system in several conditions which are conduction, convection, and radiation. Heat transfer is a science of knowledge that deals with the rate of heat energy. The modes deals in heat transfer are conduction, convection and radiation [13].

1.5 Transient Heat Transfer

Transient heat exchange is the non-consistent state exchange of energy through a medium. The transient state alludes to a non-consistent stream of vitality. This changing rate of heat exchange could be because of fluctuating temperature distinction over the medium or changing properties all through the medium.
"Transient" means the heat transfer is changing with time. The warmed side will warm first and heat will go through the material (Fourier's law of heat exchange) [14].

1.6 Previous Research

The previous research is used as a reference and guideline in this study.

1.6.1 Surface crack detection by active infrared thermography on concrete

This researcher is using the same concept where they used active thermography method in identifying the defects of cracked on the cement panel. The same technique has been used to identify the defects.

The researchers induced a short duration of pulsed thermography by meant this research also use an active thermography to detect the defect. This experiment use the short duration of heat-pulse with duration of (~3 ms). Basically, it uses the same concept of thermography where the surface cracking is detected when there is a difference contrast of heat emission between the crack and the surface. The finding results from this experimented succeed in detected the defects of 0.5 mm to 1 mm cracked width, but for the micro-crack between (0.1 mm-0.5mm) need to use another alternative to detect the contrast which is added water to the crack.

1.6.2 Previous study of surface cracks

The crack was classified based on their surface cracks, for crack widths between 0.5mm to 1 mm are considered major while for 0.1 mm to 0.5 mm are called micro-cracks. The results show that major cracks can be seen by flash stimulation while micro-cracks can only be seen after adding water. Figure 2 below shows the results obtained

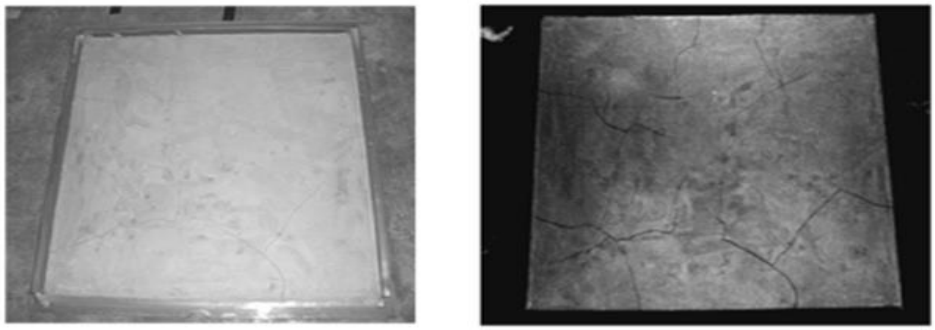

(a) (b)

Fig. 2. Image of surface cracks and thermal image [15] (a) photos of surface cracks (b) thermal image at 0.04 s after pulse

According to the results, this method is very useful for building appraisal since the maximum crack width can be investigated detailed.

2. Methodology

This experiment was done at normal surrounding temperature. Figure 3 shown the experimental setup within an enclosed area as to minimize reflected temperature from surrounding. Table 2 shows the parameter observed during the experiment.

Fig. 3. Top view of experimental setup

Table 2
Parameters of experiment inside the closed room

Parameters	Value
Emissivity of the stainless steel 304	0.95
Reflective temperature inside laboratory	30˚C
Distance between camera and model	1.0 m
Relative humidity	62%
Atmospheric temperature	26.4˚C
Surface temperature	26.1˚C
Angle of light to the subject	30˚

2.1 Experimental Procedure

Previous study focusing on surface crack by flashlight [15] has expose guidance for the current inspection. A pit-like defect [16] of fatigue failure experiment had also revealed that fatigue life to the specimen will reduce depending on its dimensions.

In this chapter, the experimental is evaluated by using active Infrared Thermography (IRT) method to inspect artificial pitted inside the pipe. This experimental conducted at close place covers with a black cloth.

The angle between source of radiation and target object was set at 30° trigonometrically. The 2 unit of 500 watts spotlight emitted radiation at a predetermine interval of time. Then, by using FLIR T640 the video was recorded. The distance between camera and surface of defects was set to 1 meter. Then, with help of FLIR Tools + Software, the video is converted to radiometric image to analyze the transient cooling rate and study the Pointed Rectangular Calibration (PRC) Pixels.

A 6 inches SCH 80, 304 stainless steel pipe with Ø10mm artificial pitting hole at 5mm depth was prepared as a model. The procedure of the thermal process begins when the radiation was produced to the surface of the pipe at an interval of time. The process of heat transfer begins with radiation mode where the heat source from spotlight tends to heat up the pipe. As heat reach the pipe surface, it changes to conduction mode, now the pipe starts to retain the heat and will discharge back the heat to the surrounding. As heat starts to discharge from the pipe, simultaneously FLIR T640 is ready to record the thermal image of the pitted.

i. The experimental model was set up and the ambient temperature and the relative humidity of surroundings are measured.
ii. The FLIR T640 camera was placed 1m distance from the model.
iii. The camera and laptop were linked together with FLIR Tools+ software to record live stream video.
iv. Both spotlights are switch on and targeted to the model until the temperature exceeds 35˚C.
v. The model was cool down back until meet the surrounding temperature.

vi. Both spotlights were switched ON, heating the model until surface temperature exceeds 35˚C. The model was left self-cooling at predetermined period of time.
vii. The experimental started with 10s of heat exposure to the model. Infrared Camera connected to PC should now in standby mode running FLIR Tools+ software.
viii. Switch OFF and isolate the spotlights while recording video.
ix. Stopped recording after 10 minutes.
x. Step 1 until 7 were repeated for 20s, 30s, 40s, 50s and 60s of heat exposure.

2.2 Analysis Procedures

i. Select suitable file at FLIR Tool+ software to be analyzed.
ii. Use Pointed Rectangular Calibration (PRC) at predetermined defect area.
iii. Played the video, while ensuring the maximum, minimum and average graph appear by selecting the plot features. Graph and data shown were based based on the location of PRC.
iv. Observe the video, a significant temperature drop can be identify by observing the highest gradient displayed upon cooling process. An initial reference line was marked for references as shown in Figure 4. The actual time in seconds, for the particular phenomenon was note down for further comparison.

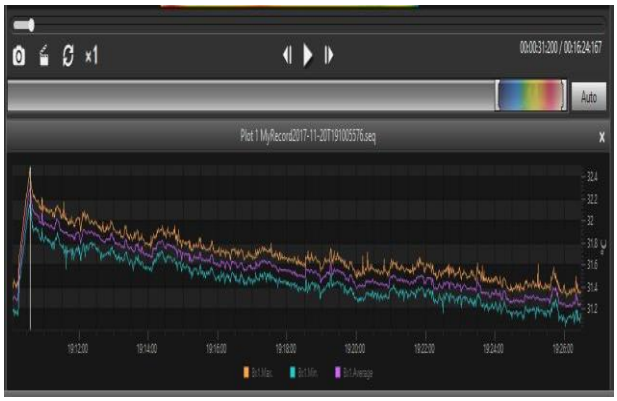

Fig. 4. Initial line for references

v. Now the radiometric image is ready for further analysis. Use a snapshot feature to save the image as shown in Figure 5 below.

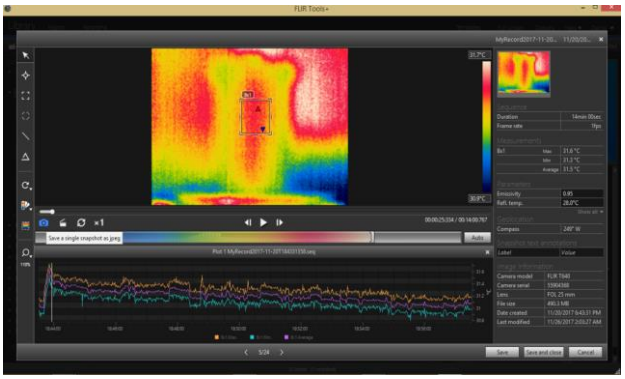

Fig. 5. Snapshot feature of the recording

vi. Each pixel of predetermine PRC radiometric image contains valuable data. Data could be extracted by converting to Comma-Separated Values (CSV) format as shown in Figure 6.

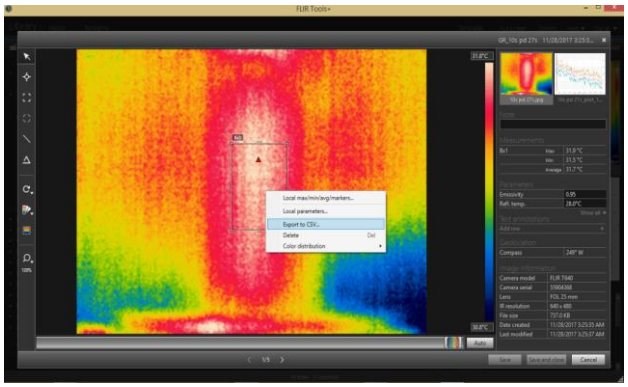

Fig. 6. Comma-Separated Values (CSV) features

vii. The PRC temperature data is tabulated in CSV format for analyses.

3. Results and Discussion

The experiment is evaluated by using active Infrared Thermography (IRT) method to inspect artificial pitted inside the pipe. This experimental conducted at enclose area.

The medium used to transfer heat via radiation to the pipe surface are using two pieces of the spotlight with power of 500 watts each. The heat emitted from the spotlight is emitted only at an interval of time. Then, by using FLIR T640 the video was recorded. The distance between camera and surface of defects is set constant to 1 meter. Then, with help of FLIR Tools+ Software, the video is converted to radiometric image to analyse the clearest image of defect occurred as to predict location, as well the interval of time and condition.

3.1 Time Interval of Radiation Exposure and Surface Temperature Monitoring

This experiment is conducted within radiation exposure of 10s, the 20s, 30s, 40s, 50s, and 60s intervals. Earlier, the pipe surface temperature were heat up to 36˚C, as to ensure procedure. The surface temperature than cool down to the surrounding temperature prior to the actual test to be conducted.

3.2 Analysis Defect in Close Room

The radiometric image was analysed with the assistance of FLR Tools+ software as to identify a significant temperature drop within highest gradient observed at cooling phase.

Figure 7 shows the graph of 20 seconds radiation exposure recorded for 16 minutes where Y axis representing surface temperature while at C Axis is representing actual times in seconds.

Figure 7 was constructed which representing maximum, minimum and average temperature at an instant within predetermined PRC radiometric image. The graph shows that surface temperature increases up to 32.5, 32.3 and 32.1°C for its maximum, minimum and average readings within 20 seconds of radiation exposure.

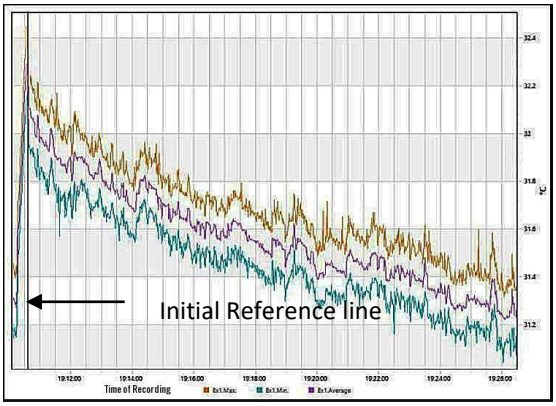

Fig. 7. Cooling phase graph of 20 seconds of radiation exposure

The analysis was done by finding the most significant temperature drop within the highest gradient observed at cooling phase. The trend of graph illustrates that, the temperature was increase to the peak upon 20 seconds of radiation exposure and shows only 2 seconds of interval for its highest gradient during cooling period.

Analysing the temperature at the critical point using FLIR Tools+ exposed that maximum temperature is 32.3˚C, average temperature 32.2˚C, and minimum temperature is 32.1˚C. Then, the cooling lines begin to uniformly decrease until the end to accommodate the surrounding temperature.

Figure 8 illustrates the radiometric image at a critical point of Initial Reference Line by using FLIR Tools+ software.

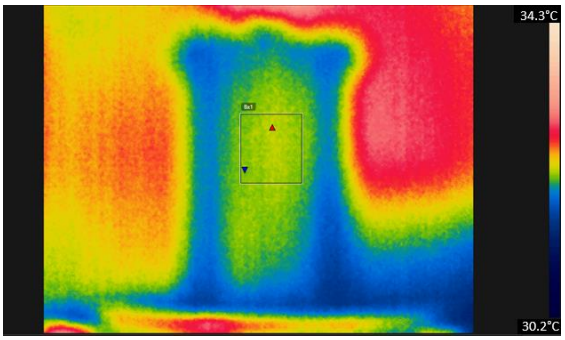

Fig. 8. Image capture at critical point of radiation exposure in the 20s

Similar with 10s and 20s of radiation exposure, all the temperature data was then represented into contour graph, as shown in Figure 9.

From the contour graph as shown in Figure 9, the defect is clearly shown and the temperature was observed between 32.5˚C and 33˚C.

At a selected PRC radiometric image, the temperature data was extracted to tabulate a contour effect. Microsoft excel chart helps to idealise the visual and contrast the chart view to allocate pitted at pipe. Black tape image at the center can be clearly seen in the chart as a reference point for emissivity checking.

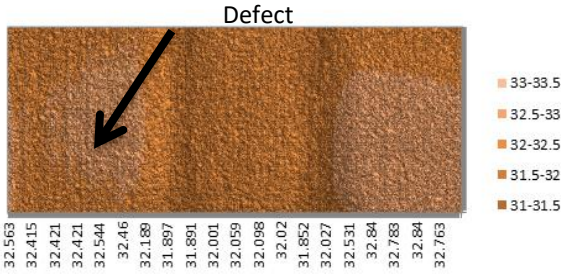

Fig. 9. Graph contour at critical point of radiation exposure in the 20s

3.3 Comparison of Results

The analysis continues to the other parameter of radiation exposure. It was compiled to understand the effect of radiation exposure and relate it to a significant temperature drop within highest gradient observed at cooling phase.

The result had revealed the time of radiation exposure will affects a significant temperature drop within highest gradient observed at cooling phase. Table 3 shows the comparison of the radiation exposure time at enclosed room.

Table 3
Time interval of significant gradient

Time of radiation expose (s)	Time interval of significant gradient appear (s)
10	7
20	2
30	1
40	Not Appear
50	Not Appear
60	Not Appear

A graph of Time Interval of Significant Gradient against Time of Radiation Exposure is constructed as shown in Figure 10.

From Figure 10, it shows the time of radiation exposes to the surface of the pipe inversely proportional to the time of pitted to appear. The significant gradient interval only appears at the state of radiation exposure within 10s, 20s and 30s while above 40s, 50s and 60s there are not capture able. Result for 30s of radiation expose show the shortest time pitted appear which is 1s of duration, for 20s of radiation expose show 2s of pitted appear while for 10s of exposure show that the longest time for the pitted appears which is 7s.

On the other hand, the accuracy of the object temperature estimated by the camera is often closely linked to the accuracy of evaluation of the input parameters. The emissivity value of the object is typically the most important parameter which needs to be determined accurately. The accuracy of the input parameters becomes less critical if the target object has high emissivity and is significantly hotter than its surroundings. As for the case of this experiments, a compensation method of known material's emissivity had been performed earlier to strengthen the results.

As a conclusion, when the exposure time of radiation decrease, longer interval of significant gradient can be observed while longer exposure of radiation will shorten the time interval of significant gradient.

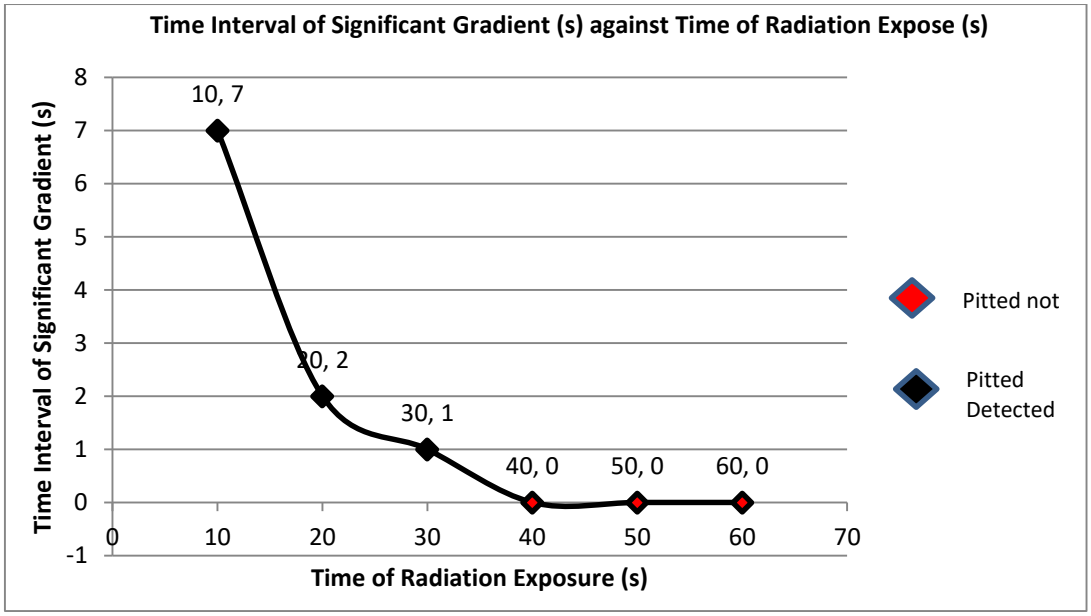

Fig. 10. Graph of time interval of significant gradient (s) against radiation exposure (s)

4. Summary and Conclusion

The research was focused on the application of active thermography for finding the location and the correspondence time of pitted will appear in steel pipe. The pipe used is stainless steel 304 as a model in this experiment, meanwhile artificially pitted is made by the drilling process. The camera will record the video in real time connected to laptop by using software FLIR Tools+ in every test of exposure. The analysis was made through the FLIR Tools+ software by analysis the graph of maximum, minimum and average temperature of the full-length video. The defect is then, represented into contour graph by extracting all the data from radiometric image.

A predetermine radiation exposure in this experiment had shown positive result to locate defect in pipe using thermal imaging within active thermography method. A different time interval of significant gradient had been revealed at each experiment conducted. Therefore, the pitted is detected based on the time of radiation exposure and surrounding temperature. The shorter time of radiation exposure will lead to longer interval of significant gradient can be achieve.

Acknowledgement

The authors thank Office for Research, Innovation, Commercialization and Consultancy Management and Universiti Tun Hussein Onn Malaysia for the financial support under Tier 1 Grant vote H 263.

References

[1] FLIR Systems Inc., *Flir T620 & T640*, 2012.

[2] Francis, R. "Galvanic corrosion of high alloy stainless steels in sea water." *British corrosion journal* 29, no. 1 (1994): 53-57. https://doi.org/10.1179/000705994798268033

[3] Javaherdashti, Reza. "Microbiologically influenced corrosion (MIC)." In *Microbiologically Influenced Corrosion*, pp. 29-79. Springer, Cham, 2017. https://doi.org/10.1007/978-3-319-44306-5_4

[4] Zhang, Xiaoge Gregory. *Corrosion and electrochemistry of zinc*. Springer Science & Business Media, 2013.

[5] Barreira, Eva, V. P. De Freitas, J. M. P. Q. Delgado, and N. M. M. Ramos. "Thermography applications in the study of buildings hygrothermal behaviour." *Infrared thermography* (2012): 171-192. https://doi.org/10.5772/28282

[6] Bagavathiappan, Subramaniam, B. B. Lahiri, T. Saravanan, John Philip, and T. Jayakumar. "Infrared thermography for condition monitoring–A review." *Infrared Physics & Technology* 60 (2013): 35-55. https://doi.org/10.1016/j.infrared.2013.03.006

[7] S. K. Dowling, M. Stewart, J. Webster, A. L. Schaefer, and T. Landgraf. "Infrared thermography for animal health and welfare monitoring: where to from here." In *Proc. 4th Aust. New Zeal. Spat. Enabled Livest. Manag. Symp.*, pp: 19., 2013.

[8] Ismon, Maznan Bin, Izzuddin Bin Zaman, and Mohd Imran Ghazali. "Condition monitoring of variable speed worm gearbox lubricated with different viscosity oils." In *Applied Mechanics and Materials*, vol. 773, pp. 178-182. Trans Tech Publications Ltd, 2015. https://doi.org/10.4028/www.scientific.net/AMM.773-774.178

[9] Ismon, Maznan, Muhd Hafeez bin Zainulabidin, Hanani binti Abd Wahab, Zaleha binti Mohamad, and Mohd Amran bin Madlan. "Thermal Gradient Pattern of Shallow Pitting Via Active Thermography–Hot Water and Steam." *International Journal of Integrated Engineering* 10, no. 1 (2018). https://doi.org/10.30880/ijie.2018.10.01.020

[10] Ismon, Maznan, and Chee Seng Ng. "Thermography analysis on welding defects and internal erosion of carbon steel pipeline." *ARPN Journal of Engineering and Applied Sciences* 11, (2016): 7498-7502.

[11] Cho, GeonHwan, Hui Tang, J. Michael Owen, and Gary D. Lock. "On the measurement and analysis of data from transient heat transfer experiments." *International Journal of Heat and Mass Transfer* 98 (2016): 268-276. https://doi.org/10.1016/j.ijheatmasstransfer.2016.03.009

[12] Manjanna, J., S. Kobayashi, Y. Kamada, S. Takahashi, and H. Kikuchi. "Martensitic transformation in SUS 316LN austenitic stainless steel at RT." *Journal of materials science* 43, no. 8 (2008): 2659-2665. https://doi.org/10.1007/s10853-008-2494-4

[13] Harde, Hermann. "Radiation and heat transfer in the atmosphere: a comprehensive approach on a molecular basis." *International Journal of Atmospheric Sciences* 2013 (2013). https://doi.org/10.1155/2013/503727

[14] Burghold, E. M., Y. Frekers, and R. Kneer. "Transient contact heat transfer measurements based on high-speed IR-thermography." *International Journal of Thermal Sciences* 115 (2017): 169-175. https://doi.org/10.1016/j.ijthermalsci.2017.01.019

[15] Sham, F. C., Nelson Chen, and Liu Long. "Surface crack detection by flash thermography on concrete surface." *Insight-Non-Destructive Testing and Condition Monitoring* 50, no. 5 (2008): 240-243. https://doi.org/10.1784/insi.2008.50.5.240

[16] M. Khattak, M. Noh, M. Tamin et al., "Effect of artificially produced pit-like defects on the strength of AISI 410 stainless steel compressor blades." *Journal of Advanced Research in Materials Science* 17, no. 1 (2016): 10-17. https://doi.org/10.11113/jt.v78.9208